

Simulation of 2D quantum transport in Ultrashort DG-Mosfets : a fast algorithm using subbands

Naoufel Ben Abdallah*, Eric Polizzi†, Mireille Mouis‡ and Florian Méhats§

* Laboratoire MIP, UMR CNRS 5640,

Université Paul Sabatier, 118 Route de Narbonne, 31062 Toulouse Cedex 4, France

Email: naoufel@mip.ups-tlse.fr

†Purdue University 1285 Electrical Engineering Building BOX 445 West-Lafayette, IN 47907-1285

‡IMEP, UMR CNRS 5130, INPG, BP 257, Grenoble, France

§Laboratoire MIP, UMR CNRS 5640,

Université Paul Sabatier, 118 Route de Narbonne, 31062 Toulouse Cedex 4, France

Abstract—A numerical method for the resolution of the two dimensional Schrödinger equation with an incoming plane wave boundary condition is proposed and applied to the simulation of ultrashort channel double gate Mosfets. The method relies on the decomposition of the wave function on subband eigenfunctions. The 2-D Schrödinger equation is then equivalent to a nondiagonal onedimensional matrix Schrödinger system. The size of the matrix being the number of considered subbands. This leads to a drastic reduction of numerical cost. The method is illustrated by simulating a squeezed channed DGMOS.

I. INTRODUCTION

As device dimensions shrink down to the quantum limit - both in the confinement direction (body or oxide thickness) and in the channel direction - it becomes more obvious that device operation will be governed by non equilibrium quantum transport phenomena (in a 2D or even 3D geometry). Source to drain tunnelling is an illustration of a full 2D quantum effect, and has been shown to become one mechanism of the degradation of device performance at ultra-short channel length (below 10nm). Simultaneously, even for the low drain voltages which are expected for such short devices, the carriers which contribute to current flow in the channel are strongly out of equilibrium, even though isotropic interactions in silicon are much more frequent than in III-V compound semiconductors. The ability of controlling drain current with a gate and of preventing drain parasitic control, will directly result from carrier out of equilibrium transport between coupled regions of the device, separated by 2D potential barriers. Therefore a self-consistent resolution of the fully two dimensional out of equilibrium Schrödinger-Poisson system is of primary importance. This subject has been widely studied in the literature and our purpose here is to propose a numerical procedure, based on the concept of subbands (see [2] for the detailed description of the method), which drastically reduces the simulation time in the case of the double-gate Mosfets.

II. THE METHOD

The geometry that we consider is bidimensional. The test case that we shall handle is the squeezed double gate MOSFET which is shown in Figure 1. In the ballistic regime the electron

density is computed by $n(x, z) = 2 \left(n_{t,l,t}(x, z) + n_{l,t,t}(x, z) + n_{t,t,t}(x, z) \right)$ where we denoted by z the transversal variable and x the parallel one and we accounted for the 6-fold degeneracy of the conduction band in silicon. The ellipsoidal symmetry of each valley was described by means of a mass tensor within the parabolic approximation. The contribution of

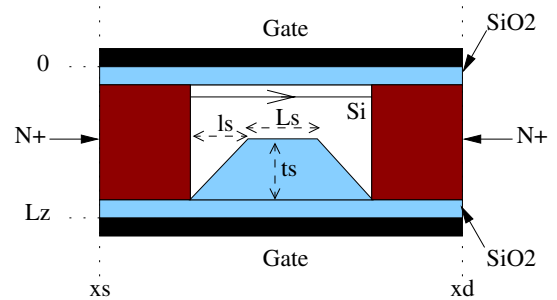


Fig. 1. Schematic view of the squeezed double gate mosfet

each valley is obtained as the density of a mixed state whose elementary states are indexed by three indices : the index p_0 of the injection port (source or drain), the index i_0 of the subband on which the electron is injected and the value k_x of the longitudinal injection wave vector. The statistics of the mixture is given by Fermi-Dirac functions with the source and drain Fermi levels [1].

To fix the ideas, the density $n_{t,l,t}$ is given by

$$n_{t,l,t}(x, z) = 2 \sum_{p_0} \sum_{i_0} \int_0^{+\infty} |\psi_{p_0, i_0, k_x}(x, z)|^2 \left(\int_{-\infty}^{+\infty} f_{FD} \left(E(p_0, i_0, k_x, k_y) - \mu_{p_0} \right) \frac{dk_y}{2\pi} \right) \frac{dk_x}{2\pi}$$

where μ_{p_0} is the fermi level of the port p_0 , the energy $E(p_0, i_0, k_x, k_y)$ is the total three dimensional energy of the electron in the valley (t, l, t) and f_{FD} is the Fermi-Dirac distribution at the lattice temperature. The elementary wave function $\psi_{p_0, i_0, k_x}(x, z)$ is a solution of the bidimensional

Schrödinger equation

$$-\frac{\hbar^2}{2m_t} \partial_x^2 \psi - \frac{\hbar^2}{2m_t} \partial_z^2 \psi + U(x, z) \psi = \varepsilon \psi$$

and the two dimensional energy ε is given by

$$\varepsilon = E(p_0, i_0, k_x, k_y) - \frac{\hbar^2 k_y^2}{2m_l} = E_{i_0}(x_{p_0}) + \frac{\hbar^2 k_x^2}{2m_t}$$

and x_{p_0} is the location of the injection port p_0 whereas E_{i_0} is the energy of the subband number i_0 defined by

$$-\frac{\hbar^2}{2m_t} \partial_z^2 \chi_i(z; x) + U(x, z) \chi_i(z; x) = E_i(x) \chi_i(z; x),$$

and U is the electrostatic potential energy. The wave function satisfies the quantum transmitting boundary conditions at the source and drain boundaries [3] while top and bottom boundaries are endowed with homogeneous Dirichlet boundary conditions.

The self-consistent simulation of the problem requires 10 iterations of the Poisson equation for the electrostatic potential. Each iteration contains the resolution of 2000 Schrödinger equation which makes the cost rather big. In order to drastically reduce the numerical cost, we notice that the subband functions χ_p constitute a complete basis for any given x . The wave function can then be written

$$\psi(x, z) = \sum_i \phi_i(x) \chi_i(z; x).$$

The ϕ_i 's solve the nondiagonal Schrödinger system

$$\begin{aligned} & -\frac{d^2}{dx^2} \varphi_\varepsilon^i(x) - 2 \sum_{j=1}^{\infty} c_{ij}^1(x) \frac{d}{dx} \varphi_\varepsilon^j(x) \\ & - \sum_{j=1}^{\infty} (c_{ij}^2(x) (\varepsilon - E_j(x))) \varphi_\varepsilon^j(x) = 0 \end{aligned}$$

where the coefficients c_{ij}^1 and c_{ij}^2 are given by

$$\begin{aligned} c_{ij}^2(x) &= \int_0^{L_z} \chi_i(z; x) \frac{\partial^2}{\partial x^2} \chi_j(z; x) dz, \\ c_{ij}^1(x) &= \int_0^{L_z} \chi_i(z; x) \frac{\partial}{\partial x} \chi_j(z; x) dz. \end{aligned}$$

The boundary conditions for this system are the one-dimensional quantum transmitting boundary conditions recovered from the two dimensional ones. After having computed the subband energies and basis functions and then solve for ϕ_i by a finite element method. The gain in the computational time comes from the replacement of the resolution of a two-dimensional equation by a system of one-dimensional equations, the computation of the subband energies being done once per Poisson iteration.

III. THE ALGORITHM

The numerical Schrödinger-Poisson algorithm is summarized by the five following steps:

- 1) For a given potential energy $U(x, z)$ on the $[x_s, x_d] \times [0, L_z]$ region, we solve the Schrödinger equations in the confined direction z for all the nodes of the transport direction with coordinate x_n , $n = 1 \dots N_x$. Therefore, we obtain N_x orthonormal sets of eigenfunctions $\{\chi_i(z)\}$

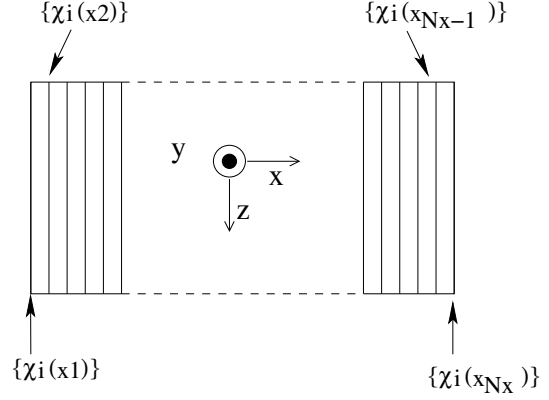


Fig. 2. The subband functions are computed for each vertical slice of the domain

and eigenvalues $\{E_i\}$ (see figure (2)). The coefficients c_{ij}^2 , c_{ij}^1 are then evaluated numerically.

- 2) For a given energy ε , the wave vectors k_i^s and k_i^d associated to the incoming scattering states in the domain on the x transport direction are calculated and the one dimensional matrix Schrödinger system is discretized using a finite element or finite difference method. The so obtained linear system is then solved either by matrix by direct methods or by iterative ones as the QMR (Quasi-Minimal Residual) procedure presented in [4].
- 3) The electron and the current densities are calculated by summing up the contribution of the elementary wave functions (indexed by their energy, injection port an injection mode, or equivalently the injection wave vector). Numerically, the upper limit on the integration over the energy variable is fixed at $\mu_p + 4k_B T$ for the port p , where μ_p is the corresponding Fermi energy.
- 4) The Poisson's equation is solved in the x, z domain using Dirichlet boundary conditions for the interfaces with the gates, and Neumann boundary conditions on the Source and Drain interfaces. The obtained real symmetric sparse system can be solved using the preconditioned conjugate gradient method.
- 5) Repeat three times all the four previous steps respectively for the different effective mass configurations. Take note that it is required only to compute two times the eigenproblem in the first step respectively for m_l^* and m_t^* on z . We so obtain two sets of eigenfunctions and eigenvalues on z along the x transport direction.

We point out some remarks related to the numerical implementation of this algorithm:

- Because of the highly non linear character of the coupled Schrödinger-Poisson system, implicit schemes have to be used for its numerical resolution. The Newton-Raphson method is not appropriate since the density depends non locally on the potential. Therefore, for a given potential V^n at the step n , we propose to implicit the scheme as follows:

$$-\nabla \left(\epsilon_r(z) \nabla V^{n+1} \right) = \frac{q}{\epsilon_0} \left(n_D(z) - n(x, z) \frac{T[V^{n+1}]}{T[V^n]} \right),$$

where T defines a functional of V (take note that ϵ_0 is the vacuum permittivity, ϵ_r is the relative dielectric constant, q denotes the free electron charge and n_D is the positive doping profile). Because of the exponential behavior of the electron density in function of the potential V , one suitable choice for T is then given by $T[V] = \exp(q\beta V)$ (with $\beta = 1/k_B T$). The linearization of this coupled system leads to the Gummel iterative scheme [5] where for a given potential V^n at the step n , the new potential V^{n+1} is now given by

$$\begin{aligned} -\nabla \left(\epsilon_r(z) \nabla V^{n+1} \right) + \frac{q}{\epsilon_0} n(x, z) \frac{V^{n+1}}{V_{ref}} \\ = \frac{q}{\epsilon_0} \left(n_D(z) - n(x, z) \left(1 - \frac{V^n}{V_{ref}} \right) \right), \end{aligned}$$

with $V_{ref} = k_B T / q$.

- In order to obtain a suitable initial guess to begin the simulations at equilibrium, one way is to use the well known Thomas-Fermi/Poisson semi-classical approximation, then

$$n(x, z) = 2 \int \int \int_{-\infty}^{+\infty} f_{FD}(E - \mu) \frac{dk_x dk_y dk_z}{8\pi^3},$$

where the wave functions are plane waves in the whole domain and the energy depends on the local potential

$$E = U(x, z) + \frac{\hbar^2}{2} \left(\frac{k_x^2}{m_x^*} + \frac{k_y^2}{m_y^*} + \frac{k_z^2}{m_z^*} \right),$$

where we have again to sum over the three different mass configurations. In the present case the coupled system will be solved using a Newton-Raphson method. However, a better choice for the initial guess consists in taking into account of the confinement of the electron gas in the z direction using the $\chi_i(z; x)$ functions [6]. The electron density of this hybrid model is written as

$$n(x, z) = 2 \sum_i \int_{-\infty}^{+\infty} |\chi_i(z; x)|^2 \left(\int_{-\infty}^{+\infty} f_{FD}(E - \mu) \frac{dk_y}{2\pi} \right) \frac{dk_x}{2\pi},$$

with

$$E = E_i(x, z) + \frac{\hbar^2}{2} \left(\frac{k_x^2}{m_x^*} + \frac{k_z^2}{m_z^*} \right).$$

- If the thickness of the Silicon layer is large enough ($\sim 10\text{nm}$ or more) then the first two modes $\chi_1(z; x)$ and $\chi_2(z; x)$ are separate and their energies are very close to each other. In this case, all the numerical procedures that we could use to solve each independent eigenvalue problems on z along the x transport direction (see figure (2)), appear not suitable in order to keep the regularity of

the function χ_1 and χ_2 on x . Our method then produces the first two eigenvalues in a randomized order and the eigenfunctions have a randomized sign as shown in Figure (3), the final result on $[x_s, x_d] \times [0, L_z]$ is wrong.

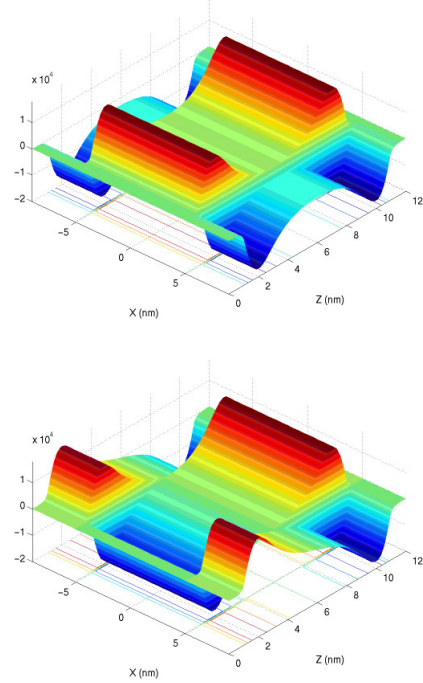


Fig. 3. Variations of the first two eigenfunctions $\chi_1(z; x)$ (on the left) and $\chi_2(z; x)$ (on the right) along the x transport direction. In this case (we take 10nm both for the thickness and the length of the channel), we note that the eigenfunctions show a non regular behavior in the middle of the device.

To cope with this problem, we treat the two first eigenvalues as a single degenerate eigenvalue and rotate the eigenfunction by a suitable amount which lets them depend smoothly on x . For further details we refer to [1]. Figure (4) is given to illustrate the variations of the first two eigenfunctions after we have applied the suitable rotation.

IV. COMMENTS

Let us mention that contrary to the reference [7] where the off-diagonal terms accounting for subband coupling are not taken into account, fully bidimensional effects are fully taken into account since the coupled subband system is equivalent to the dimensional Schrödinger equation. In particular our method handles the squeezed DG MOSFET. In the figures below, we show how the wave function is partly transferred from the first subband in the source port to the second subband in the drain port and how the coupling terms modify the source-to-drain I-V curve.

As a conclusion, the method that we have presented is equivalent to the resolution of the fully bidimensional Schrödinger equation while having a much lower numerical cost (by a factor 10). It allows to compute I-V characteristics

of the double Gate Mosfets in a reasonable computation time and is promising for three-dimensional simulations.

ACKNOWLEDGMENT

The authors acknowledge support from the Centre national de la Recherche Scientifique (action spécifique MathSTIC). This work was performed while the second author was member of the MIP laboratory (Toulouse).

REFERENCES

- [1] E. Polizzi, N. Ben Abdallah, Phys. Rev B. **66**, 245301-245309 (2002).
- [2] E. Polizzi, N. Ben Abdallah, in preparation.
- [3] C.S. Lent and D.J. Kirkner, J. Appl. Phys. **67**, 6353 (1990).
- [4] R.W. Freund, SIAM J. Sci. Stat. Comput. **12**, 425 (1992).
- [5] H.K. Gummel, IEEE Trans. on Elec. Dev., **11**, 455 (1964).
- [6] A.S. Spinelli, A. Benvenuti and A. Pacelli, IEEE Trans. on Electron Devices **45**, 1342 (1998).
- [7] R. Venugopal, Z. Ren, S. Datta, M.S. Lundstrom and D. Jovanovic, J. Appl. Phys. **92**, 3730 (2002).

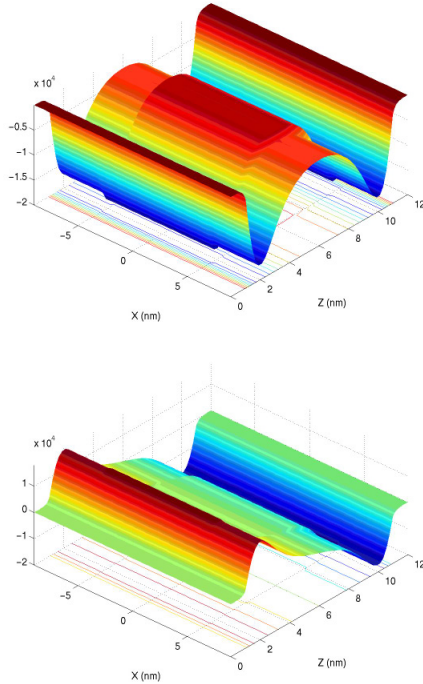


Fig. 4. Variations of the first two eigenfunctions $\chi_1(z; x)$ (on the left) and $\chi_2(z; x)$ (on the right) along the x transport direction numerically obtained using the assumption of degenerate states. We note now a regular behavior for the eigenfunctions in the device.

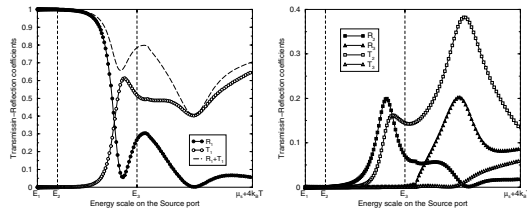


Fig. 5. Reflection and transmission coefficients from the first subband into the first subband (on the left) and on higher subbands (on the right) as function of the energy. The results are obtained for an incoming wave on the first subband.

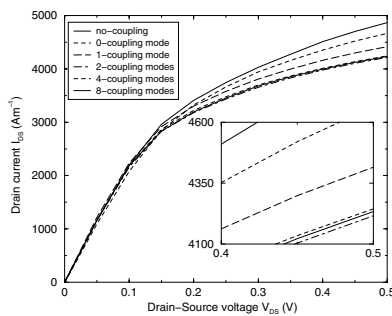


Fig. 6. I-V characteristics for the device with squeezed channel where different modes coupling configurations are presented.